

2000-08-07

Self-assembled zinc blende GaN quantum dots grown

Martínez-Guerrero, Esteban; Adelman, Christoph; Chabuel, F.; Simon, Julia; Pelekanos, N.T.; Mula, Guido; Daudin, B.; Feuillet, G.; Mariette, H.

E. Martinez-Guerrero, C. Adelman, F. Chabuel, J. Simon, N. T. Pelekanos, Guido Mula,a) B. Daudin, G. Feuillet, and H. Mariette, Self-assembled zinc blende GaN quantum dots grown, APPLIED PHYSICS LETTERS Vol. 77, N. 6, pp 809 - 811, (2000)

Enlace directo al documento: <http://hdl.handle.net/11117/652>

Este documento obtenido del Repositorio Institucional del Instituto Tecnológico y de Estudios Superiores de Occidente se pone a disposición general bajo los términos y condiciones de la siguiente licencia:
<http://quijote.biblio.iteso.mx/licencias/CC-BY-NC-ND-2.5-MX.pdf>

(El documento empieza en la siguiente página)

Self-assembled zinc blende GaN quantum dots grown by molecular-beam epitaxy

E. Martinez-Guerrero, C. Adelman, F. Chabuel, J. Simon, N. T. Pelekanos, Guido Mula,^{a)} B. Daudin, G. Feuillet, and H. Mariette^{b)}

CEA-CNRS Joint Group "Nanophysique et Semiconducteurs," Département de Recherche Fondamentale sur la Matière Condensée, SPMM, 17 Rue des Martyrs, 38054 Grenoble Cedex 9, France

(Received 20 April 2000; accepted for publication 12 June 2000)

Zinc blende (ZB) GaN quantum dots have been grown by plasma-assisted molecular-beam epitaxy on AlN buffer layers using 3C-SiC(001) substrates. The two- to three-dimensional growth mode transition is studied by following the evolution of the reflection high-energy electron diffraction pattern. ZB GaN island layers are further examined by atomic force microscopy and transmission electron microscopy, extracting a mean island height of 1.6 nm and a mean diameter of 13 nm at a density of $1.3 \times 10^{11} \text{ cm}^{-2}$. Embedded ZB GaN quantum dots show strong ultraviolet photoluminescence without any thermal quenching up to room temperature. © 2000 American Institute of Physics. [S0003-6951(00)01032-9]

The current interest in self-assembled semiconductor quantum dots (QDs) is partly motivated by the potential to achieve lasers with low threshold currents and improved temperature characteristics.¹ Moreover, the nanometric size and the coherent growth of self-assembled QDs are particular advantages in situations where the surrounding crystal matrix disposes of a large number of structural defects. This is the case of group III nitrides which generally exhibit high threading dislocation densities of the order of $10^8 - 10^{10} \text{ cm}^{-2}$.

To date, self-assembled group III nitride QDs have been grown exclusively in the wurtzite (WZ) structure; for the GaN/AlN system, such QDs have been achieved both by metalorganic chemical vapor deposition (CVD)² as well as molecular-beam epitaxy (MBE) using Stranski-Krastanow growth mode.^{3,4}

Despite the above-mentioned achievements for the WZ phase of nitrides, its zinc blende (ZB) counterparts present additional interest due to the absence of internal electric fields. It has been established that the optical properties of WZ GaN/AlGaIn quantum wells⁵⁻⁷ and GaN/AlN QDs^{8,4} are strongly influenced by the presence of a huge internal electric field. This internal field, which can reach several MV/cm, stems from both spontaneous polarization and piezoelectric effects since WZ nitride samples are usually grown along the polar [0001] axis. For optoelectronic applications, the existence of the field can be detrimental since it brings about low exciton oscillator strengths and, consequently, long radiative lifetimes, ensuing from spatial separation of electrons and holes.

In contrast, ZB nitride structures are usually grown along the nonpolar [001] axis on GaAs(001)⁹⁻¹¹ or 3C-SiC(001)^{9,12} substrates, so that no internal field is present in heterostructures. Then, the above-mentioned problems

can, in principle, be eluded. It is the aim of the present letter to demonstrate that self-assembled GaN QDs in the ZB phase can be grown by MBE.

The samples were grown in a commercial MECA 2000 MBE growth chamber equipped with Ga and Al effusion cells. Active N was generated by a radio-frequency plasma cell from EPI company. The substrate consisted of a 3- μm -thick 3C-SiC(001) layer grown by CVD on Si(001).

Before GaN deposition, ZB AlN buffer layers have been grown at substrate temperatures of $T_S = 720^\circ\text{C}$ and growth rates of 300 nm/h. The reflection high-energy electron diffraction (RHEED) pattern was found to be streaky after the deposition of about 5 nm, showing no WZ traces during nucleation. A RHEED image of such a smooth AlN buffer layer is shown in Fig. 1(a).

The growth mode experienced by ZB GaN on AlN at $T_S = 720^\circ\text{C}$ was studied by RHEED. Figures 1(a)–1(c) show the evolution of the RHEED pattern during GaN deposition:

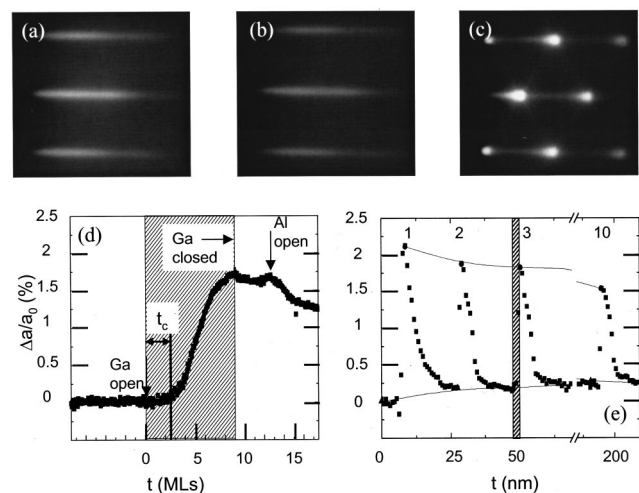


FIG. 1. Evolution of the RHEED pattern during GaN deposition on AlN. (a) Zinc blende AlN buffer. (b) GaN wetting layer. (c) GaN islands. Variation of the in-plane lattice parameter a during the growth of (d) a single layer of GaN islands and (e) a ten-period multilayer sample (the numbers label the layer order). Where shown, the shaded areas correspond to GaN deposition.

^{a)}Permanent address: INFN and Dipartimento di Fisica, Università di Cagliari, Cittadella Universitaria, Strada Provinciale Monserrato-Setzu km 0.7, 09042 Monserrato, Cagliari, Italy.

^{b)}Also at: Laboratoire de Spectrométrie Physique, Université Joseph Fourier Grenoble I, France.

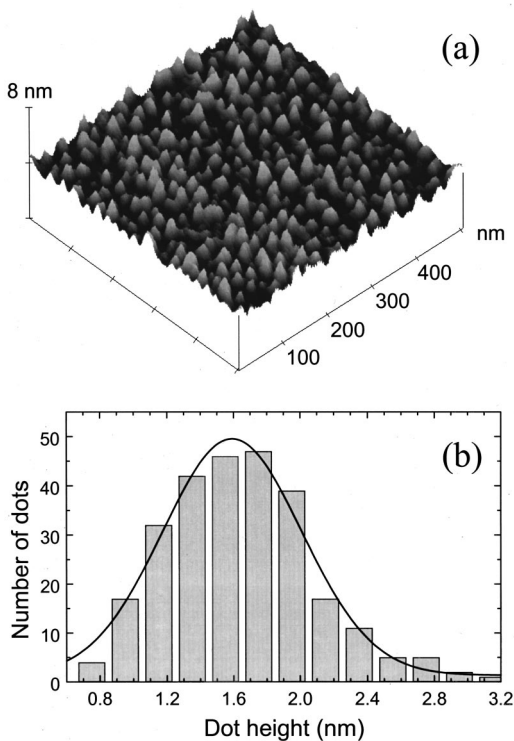


FIG. 2. (a) Topographic AFM image of a single GaN QD surface layer. (b) Distribution of the GaN island height above the wetting layer as extracted from AFM measurements.

starting from a smooth AlN layer [Fig. 1(a)], the RHEED image remains streaky during the initial stage of GaN growth [Fig. 1(b)], but changes abruptly after 2–3 monolayers (ML) to a superposition of streaks and Bragg spots [Fig. 1(c)], which is ascribed to GaN islanding. Note the appearance of weak $\{111\}$ facets.

These GaN islands were subsequently overgrown with AlN, recovering a smooth surface after typically 15 nm, as indicated by a streaky RHEED pattern, similar to that depicted in Fig. 1(a). By repeating this cycle, multilayer samples were achieved. Raman and x-ray diffraction measurements ascertain the ZB phase purity of these samples.¹²

To further investigate the RHEED observations, real-time measurements of the in-plane lattice parameter a were performed by recording the relative variation of the RHEED streak separation $\Delta a/a_0$ with respect to the initial AlN lattice parameter a_0 . For fully relaxed GaN on AlN, $\Delta a/a_0$ equals 2.7% using the values of $a_{\text{AlN}}=a_0=4.38 \text{ \AA}$ (Ref. 13) and $a_{\text{GaN}}=4.50 \text{ \AA}$ (Ref. 14). Figure 1(d) shows the variation of $\Delta a/a_0$ during the growth of a GaN island layer, subsequently capped by AlN. In keeping with the RHEED pattern, no variation of the in-plane lattice parameter is observed for the first 2–3 ML. Thereafter, correlated to the appearance of Bragg spots, $\Delta a/a_0$ increases rapidly to a level of about 1.7%, attributed to relaxation by free surface formation on the islands.

Finally, Fig. 1(e) shows the variation of $\Delta a/a_0$ during the growth of a ten-period multilayer sample. During AlN overgrowth of the GaN islands, $\Delta a/a_0$ decreases progressively, reaching the initial fully relaxed level after about 10 nm. The reversibility of the relaxation further corroborates the interpretation of elastic relaxation by GaN islanding, as expected for Stranski–Krastanow growth. As a whole, one

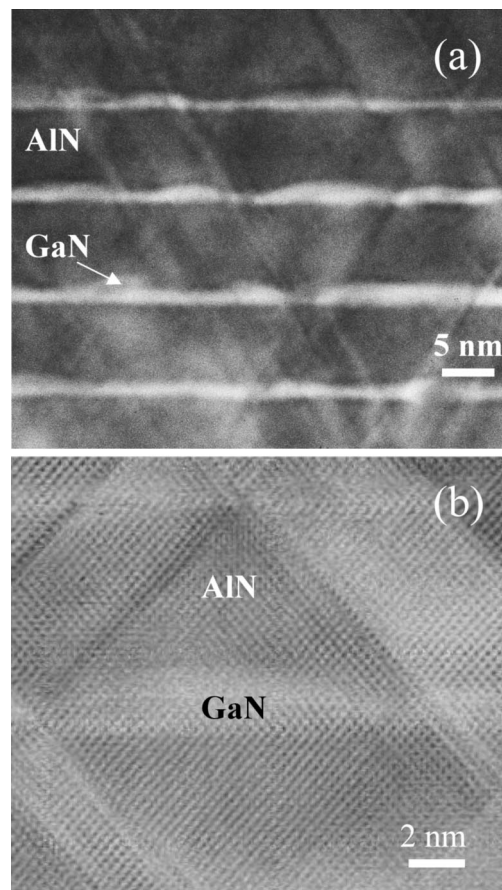


FIG. 3. (a) Dark-field cross-sectional TEM image of four layers of GaN islands. (b) High-resolution TEM image of a single GaN island surrounded by $\{111\}$ stacking faults.

observes a good reproducibility of the growth cycle. Note however, that the maximum relaxation slightly decreases with higher layer numbers. The explanation for this behavior remains unclear at the moment.

The GaN island formation evidenced by RHEED has been further examined by two techniques: first, GaN islands surface layers were analyzed by atomic force microscopy (AFM) and, second, multilayer samples were investigated by transmission electron microscopy (TEM).

Figure 2 shows a topographic AFM image of a single GaN island layer grown on a 10-nm-thick AlN buffer layer. The extracted average island height *above the wetting layer* is $1.6 \pm 0.5 \text{ nm}$. The average dot diameter is 13 nm, at a density of $1.3 \times 10^{11} \text{ cm}^{-2}$. This leads to an aspect ratio of about 1/8, in contrast to a value of 1/5 in the case of WZ GaN quantum dots.³ This is much smaller than the aspect ratio value of $1/\sqrt{2}$ expected for pyramids formed by $\{111\}$ facets, as observed by RHEED, therefore the GaN islands are truncated.

Following Ref. 15, the relaxation of an island can be approximately written as a function of the ratio of its height h and diameter d only as

$$\epsilon_{xx}(h) = \epsilon_{xx}(0) \left(1 - \frac{2\pi h}{d} \right), \quad (1)$$

where $\epsilon_{xx}(h)$ and $\epsilon_{xx}(0)$ are the deformations on the top and at the bottom of the nanostructure, respectively. Applying this formula, we obtain a residual deformation in our ZB

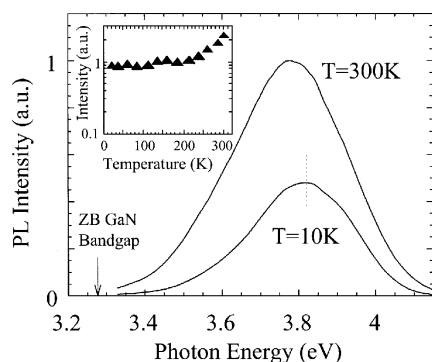


FIG. 4. Photoluminescence spectra of a ten-period multilayer sample at 10 and 300 K. The inset shows the spectrally integrated PL intensity as a function of sample temperature.

GaN islands corresponding to a partial relaxation equivalent to $\Delta a/a_0 = 2.1\%$, in good agreement with the RHEED data [see Fig. 1(e)]. Note that the same approach applied to our WZ GaN islands leads to complete relaxation of the in-plane lattice parameter, as also observed experimentally.¹⁶

A $(\bar{1}10)$ cross-sectional TEM dark-field image in Fig. 3(a) clearly reveals that the GaN islands are formed on top of a two-dimensional wetting layer. Although it is difficult to deduce the wetting layer thickness from these images, the 2–3 ML estimated from RHEED data are in qualitative agreement. Furthermore, the size of the GaN QDs agrees fairly well with that measured by AFM. One can also notice the presence of numerous stacking faults along the $\{111\}$ planes. The high-resolution TEM image in Fig. 3(b) shows that the islands grow preferentially within each domain bounded by these stacking faults. The large density of stacking faults may be at the origin of the broad size distribution of the islands since they can lead to local relaxation at the growth front and, thus, to an inhomogeneous strain distribution on the surface.

In Fig. 4 we compare the photoluminescence (PL) spectra of a stack of ten QD layers embedded in AlN at $T = 10$ K and $T = 300$ K, illuminated by 10 W/cm^2 of a frequency-tripled Ti-sapphire laser with $\lambda_X = 266 \text{ nm}$ ($E_X = 4.67 \text{ eV}$). For this photon energy, the GaN QDs are excited by absorption directly in the QD excited states. The energy shift of the maximum of the PL line between 10 and 300 K corresponds exactly to the variation of the bulk ZB GaN band gap¹⁷ for this temperature range. The PL peak is typically centered at 3.8 eV, blueshifted by more than 500 meV with respect to the bulk ZB GaN band gap ($E_g = 3.26 \text{ eV}$ at 10 K). This confinement energy is much stronger than that of small WZ GaN QDs,⁸ confirming the absence of strong electric fields in these ZB nanostructures.

The PL spectral shape and the linewidth remain practically unchanged with temperature, which is consistent with intrinsic QD PL emission coming from an ensemble of uncoupled QDs. Moreover, the linewidth of the broad luminescence spectra is in agreement with the large dispersion of the dot size revealed by both AFM and TEM measurements.

The inset in Fig. 4 shows the spectrally integrated PL intensity as a function of the sample temperature. As expected for QDs, no thermal quenching of the PL intensity is observed up to room temperature. Surprisingly, the intensity rather increases by a factor of 2 between 200 and 300 K. This could be a consequence of an increase in the absorption coefficient of QDs at the excitation wavelength, resulting from the decrease of the GaN band gap energy at higher temperatures.

In conclusion we have demonstrated that growth of ZB GaN on AlN at $T_S = 720^\circ \text{C}$ follows a Stranski–Krastanow mode. As a consequence, we have grown ZB GaN QDs with a mean diameter of 13 nm and a mean height of 1.6 nm above the wetting layer. The QDs show strong ultraviolet PL emission that is blueshifted with respect to the ZB bulk GaN band gap energy. Furthermore, the emission energy is higher than that of WZ GaN QDs of the same height, even though the GaN band gap is smaller for the ZB than for the WZ structure. This supports the absence of a large internal electric field in ZB nanostructures. The PL intensity is found to persist up to room temperature, as expected for zero-dimensional confinement.

The authors are very grateful to P. Aoughé-Nzé and Y. Monteil (Université Claude Bernard, Lyon) for providing the SiC substrates. E. Martinez-Guerrero acknowledges CONACYT-Mexico and SFERE-France for financial support.

- ¹Y. Arakawa and H. Sakaki, *Appl. Phys. Lett.* **40**, 939 (1982).
- ²S. Tanaka, S. Iwai, and Y. Aoyagi, *Appl. Phys. Lett.* **69**, 4096 (1996).
- ³B. Daudin, F. Widmann, G. Feuillet, Y. Samson, M. Arlery, and J. L. Rouvière, *Phys. Rev. B* **56**, R7069 (1997); F. Widmann, B. Daudin, G. Feuillet, Y. Samson, J. L. Rouvière, and N. T. Pelekanos, *J. Appl. Phys.* **83**, 7618 (1998).
- ⁴B. Damlano, N. Grandjean, F. Semond, J. Massies, and M. Leroux, *Appl. Phys. Lett.* **75**, 962 (1999).
- ⁵J. S. Im, H. Kollmer, J. Off, A. Sohmer, F. Scholz, and A. Hangleiter, *Phys. Rev. B* **57**, R9435 (1998).
- ⁶M. Leroux, N. Grandjean, J. Massies, B. Gil, P. Lefebvre, and P. Bigenwald, *Phys. Rev. B* **60**, 1496 (1999).
- ⁷J. Simon, R. Langer, A. Barski, and N. T. Pelekanos, *Phys. Rev. B* **61**, 7211 (2000).
- ⁸F. Widmann, J. Simon, B. Daudin, G. Feuillet, J. L. Rouvière, N. T. Pelekanos, and G. Fishman, *Phys. Rev. B* **58**, R15 989 (1998).
- ⁹H. Okumura, K. Ohta, G. Feuillet, K. Balakrishnan, S. Chichibu, H. Hamaguchi, P. Hacke, and S. Yoshida, *J. Cryst. Growth* **178**, 113 (1997).
- ¹⁰O. Brandt, H. Yang, A. Trampert, W. Wassermeier, and K. H. Ploog, *Appl. Phys. Lett.* **71**, 473 (1997).
- ¹¹D. J. As, T. Simonsmeier, B. Schoettker, T. Frey, D. Schikora, W. Kriegseis, W. Burkhardt, and B. K. Meyer, *Appl. Phys. Lett.* **73**, 1835 (1998).
- ¹²B. Daudin, G. Feuillet, J. Hübner, Y. Samson, F. Widmann, A. Philippe, C. Bru-Chevallier, G. Guillot, E. Bustarret, G. Bentoumi, and A. Deneuve, *J. Appl. Phys.* **84**, 2295 (1998).
- ¹³I. Petrov, E. Mojab, R. C. Powell, and J. E. Greene, *Appl. Phys. Lett.* **60**, 2491 (1992).
- ¹⁴S. Strite, J. Ruan, Z. Li, A. Salvador, H. Chen, D. J. Smith, W. J. Choyce, and H. Morkoç, *J. Vac. Sci. Technol. B* **9**, 1924 (1991).
- ¹⁵R. Kern and P. Müller, *Surf. Sci.* **392**, 103 (1997).
- ¹⁶C. Adelman, G. Mula, G. Feuillet, and B. Daudin (unpublished).
- ¹⁷J. Petalas, S. Logothetidis, S. Bouladakis, M. Alouani, and J. M. Wills, *Phys. Rev. B* **52**, 8082 (1995).